

## ACTIVE FAULT TOLERANT CONTROL OF NONLINEAR SYSTEMS: THE CART-POLE EXAMPLE

MARCELLO BONFÈ \*, PAOLO CASTALDI \*\*, NICOLA MIMMO \*\*, SILVIO SIMANI \*

\* Department of Engineering  
University of Ferrara, Via Saragat 1/E, 44124 Ferrara, Italy  
e-mail: {silvio.simani, marcello.bonfe}@unife.it.

\*\*Department of Electronics, Computer Science and Systems  
University of Bologna, Via Fontanelle 40, 47100 Forlì, Italy  
e-mail: {paolo.castaldi, nicola.mimmo2}@unibo.it.

This paper describes the design of fault diagnosis and active fault tolerant control schemes that can be developed for nonlinear systems. The methodology is based on a fault detection and diagnosis procedure relying on adaptive filters designed via the nonlinear geometric approach, which allows obtaining the disturbance de-coupling property. The controller reconfiguration exploits directly the on-line estimate of the fault signal. The classical model of an inverted pendulum on a cart is considered as an application example, in order to highlight the complete design procedure, including the mathematical aspects of the nonlinear disturbance de-coupling method based on the nonlinear differential geometry, as well as the feasibility and efficiency of the proposed approach. Extensive simulations of the benchmark process and Monte Carlo analysis are practical tools for assessing experimentally the robustness and stability properties of the developed fault tolerant control scheme, in the presence of modelling and measurement errors. The fault tolerant control method is also compared with a different approach relying on sliding mode control, in order to evaluate benefits and drawbacks of both techniques. This comparison highlights that the proposed design methodology can constitute a reliable and robust approach for application to real nonlinear processes.

**Keywords:** fault detection and isolation, nonlinear filter, nonlinear geometric approach, fault-tolerant control, cart-pole nonlinear model.

### 1. Introduction

Feedback control systems for mechatronic engineering applications strongly rely on actuators, sensors and data acquisition/interface components to ensure a proper interaction between the physical controlled system and control devices. Faulty conditions of those system components lead to a drastic reduction or loss of stability and performance properties, which may even cause damages to the physical system. Therefore, there is a growing demand for reliability, safety and fault tolerance in control systems for mechatronics. It is necessary to design control systems which are capable of tolerating potential faults in order to improve the reliability and availability, while providing a desirable performance.

These types of control systems are often known as fault-tolerant control systems, which possess the ability to accommodate component faults automatically. They are

capable of maintaining the overall system stability and acceptable performance in the event of such faults. In other words, a closed-loop control system which can tolerate component malfunctions while maintaining desirable performance and stability properties is said to be a *fault-tolerant control system*. As shown in Fig. 1, fault-tolerant control system design is based on a Fault Detection and Diagnosis (FDD) scheme. Thus, since fault identification is important, FDD is mainly used to highlight the requirement of fault estimation.

Over the last three decades, the growing demand for safety, reliability, maintainability, and survivability in technical systems has triggered off significant research in FDD. Such efforts have led to the development of many FDD techniques; see, e.g., the survey works by Simani *et al.* (2003), Mahmoud *et al.* (2003), Korbicz *et al.* (2004), Blanke *et al.* (2006), Isermann (2005), Witczak (2007), Zhang and Jiang (2008), Ding (2008), Benini *et al.*

(2009), Theilliol *et al.* (2008), Li *et al.* (2007) or Rodrigues *et al.* (2007).

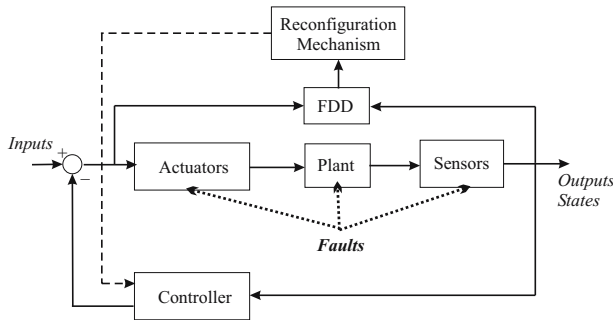


Fig. 1. Schematic diagram for the AFTCS with an actuator, plant components, and sensor faults.

In general, fault tolerant control methods are classified into two types, i.e., Passive Fault Tolerant Control Schemes (PFTCSs) and Active Fault Tolerant Control Schemes (AFTCSs) (Mahmoud *et al.*, 2003; Blanke *et al.*, 2006; Zhang and Jiang, 2008; Noura *et al.*, 2009; Edwards *et al.*, 2010).

In PFTCSs, controllers are fixed and designed to be robust against a class of presumed faults. This approach needs neither FDD schemes nor controller reconfiguration, but it has limited fault-tolerant capabilities (Mahmoud *et al.*, 2003; Zhang and Jiang, 2008). In contrast to PFTCSs, AFTCSs react to system component failures actively by reconfiguring control actions so that the stability and acceptable performance of the entire system can be maintained.

A successful AFTCS design relies heavily on real-time FDD schemes to provide the most up-to-date information about the true status of the system. Therefore, the main goal in a fault-tolerant control system is to design a controller with a suitable structure to achieve stability and satisfactory performance, not only when all control components are functioning normally, but also in cases when there are faults in sensors, actuators, or other system components.

Regarding AFTCS design, Zhang and Jiang (2008) argued that, in an AFTCS, good FDD is needed. They claim that, for the system to react properly to a fault, timely and accurate detection and location of the fault are needed. The most researched area in fault diagnosis is the residual generation approach using dynamic observers or filters. Plant-model mismatches can cause false alarms or, even worse, missed faults. Robustness issues in FDD are therefore very important (Chen and Patton, 1999; Blanke *et al.*, 2006; Isermann, 2005; Witczak, 2007).

This paper is focused on the development of a novel AFTCS that integrates a reliable and robust fault diagnosis scheme with the design of a controller reconfiguration system. In particular, the methodology is based on a fault

detection and diagnosis procedure relying on adaptive filters designed via the nonlinear geometric approach. The controller reconfiguration exploits a second control loop, depending on the on-line estimate of the fault signal. One of the advantages of this strategy is that, for example, the structure of logic-based switching controller is not required.

The novelty of the proposed AFTCS lies in the feedback of the estimated fault signal, which is obtained by adaptive filters designed via the nonlinear geometric approach. The achieved simulation results show how the closed loop of a reconstructed fault signal not only enhances the feedback itself, but also improves the final performances of the overall system. Compared with different fault tolerant approaches, (e.g., Marcos *et al.*, 2005), the suggested AFTCS strategy can maintain performance with significant actuator faults, since these signals are reconstructed by the FDD logic with good accuracy.

Concerning the FDD procedure, the paper describes a nonlinear scheme which provides the fault detection, isolation and fault size estimation. The FDD nonlinear method is based on the NonLinear Geometric Approach (NLGA) developed by De Persis and Isidori (2001). By means of this framework, a disturbance de-coupled adaptive nonlinear filter providing fault identification is developed. It is worth observing that the original NLGA FDD scheme based on residual signals cannot provide, in general, fault size estimation.

Both the NLGA Adaptive Filters (NLGA-AF) and the AFTCS strategy are applied to the well-known model of an inverted pendulum on a cart (also called a cart-pole system), an underactuated mechanical structure that is commonly used as a benchmark system for control design and mechatronics prototyping. A simulation model for the complete AFTCS loop has been implemented in the Matlab<sup>®</sup> and Simulink<sup>®</sup> environments, and tested in the presence of actuator faults, disturbances, measurement noise and modelling errors. The achieved results in faulty conditions show asymptotic fault accommodation and control objective recovery.

The proposed robustness and stability analysis methodology is based on selected performance indices, such as the mean squared reconstruction error and the tracking error, which depend on the capabilities of the AFTCS strategy. As this work deals also with the analysis of the suggested AFTCS methodology, when applied to the cart-pole benchmark system, economic cost software algorithms to determine the overall performances of the proposed method are described and implemented in the Matlab<sup>®</sup> and Simulink<sup>®</sup> environments. They exploit a detailed simulation of the cart-pole nonlinear model, with different control strategies can be applied, and subject to disturbance signals, model uncertainty and measurement noise processes.

The initial performance analysis is carried out by ap-

plying the suggested AFTCS to the nonlinear benchmark controlled via a simple Linear Quadratic Regulator (LQR) designed for the linearized model of the inverted pendulum on a cart. Secondly, the model of the system is simulated in connection with a *Sliding Mode Controller* (SMC).

This comparison appears quite important, as the SMC is an established method of controlling uncertain dynamical systems (Utkin, 1977; 1992; Edwards and Spurgeon, 1998). Its invariance properties with respect to the so-called matched uncertainty have encouraged researchers to apply sliding mode techniques to a wide variety of application areas (Slotine and Sastry, 1983; Utkin, 1992; Su and Stepanenko, 1994; Edwards and Spurgeon, 1998; Edwards, 2004). The early theory was developed within a state-space framework and invariably assumed that full state information was available for use in the control law. The design of a (state feedback) SMC traditionally involves first the selection of a sliding surface, so that the associated reduced order sliding motion has appropriate dynamics, then the design of a control law to induce and maintain a sliding motion. Many approaches have been proposed for the design of the sliding surface—these include pole placement, eigenstructure assignment, optimal quadratic and Linear Matrix Inequality (LMI) methods (Utkin, 1992; Edwards and Spurgeon, 1998; Edwards, 2004). The approach based on SMC schemes shows that it is able to handle faults without reconfiguring the overall structure of the controller. Even if the controller is relatively simple, it can work in several operating points without any gain scheduling, while maintaining performance with actuator faults without explicitly detecting them. In such a way, it is possible to analyse, verify and compare the robustness and the stability of the proposed AFTCS.

In particular, since the final AFTCS design relies on both fault signal estimation and the disturbance decoupling, it is necessary to evaluate the impact of modelling uncertainties, disturbance and measurement errors on the AFTCS system. The overall AFTCS scheme verification uses extensive Monte Carlo simulations for the analysis and assessment of design, robustness, stability, and its final performance evaluation. This study also describes simulated verification that this comprehensive methodology can constitute a viable approach for real application of the suggested AFTCS strategy.

It is worth noting that the paper presents a fault diagnosis method oriented to the design of an AFTCS, which was already developed in works by the same authors, but applied to aerospace examples (Bertoni *et al.*, 2010a; 2010b; Baldi *et al.*, 2010). However, the contribution of the paper consists of the application of the AFTCS scheme to a well-known benchmark, in order to highlight the computational and mathematical aspects of nonlinear disturbance decoupling design, which are particularly difficult

in the case of the benchmark considered; hence it can be considered also a tutorial for researchers working in FDD as well as FTC. It can be also observed that, for the first time, the presented disturbance decoupling problem has been solved for the cart-pole system. This represents the first contribution of the paper. Moreover, with reference to the achieved performances of the overall fault tolerant control scheme, the advantages and drawbacks of the complete design scheme applied to the nonlinear inverted pendulum example are also discussed and compared with reference to widely used control strategies. In particular, two schemes have been used, namely, the LQR and the SMC.

Note also how the proposed fault tolerant scheme allows maintaining the existing controller, since a further loop is added to the original scheme, thus providing in the faulty case the feedback of the fault estimate provided by the nonlinear geometric approach fault diagnosis module. Many applications require not to change or modify the existing controllers. With reference to the proposed benchmark, the LQR is not fault tolerant, while the SMC presents intrinsic fault tolerant capabilities. Thus, the LQR acquires fault tolerant characteristics when the further loop is implemented. In the authors' opinion, this point represents an important feature of the proposed FTC scheme.

Finally, it is important to highlight that the final performances of the proposed FTC strategy are mainly due to the fault estimate that is unbiased thanks to the disturbance decoupling method.

The work is organised as follows. Section 2 provides the description of the cart-pole nonlinear benchmark system. The analysis of the models for actuator fault and disturbance signals acting on the systems is also performed. Section 3 describes the implementation of the FDD scheme and the structure of the AFTCS strategy. The achieved results are reported in Section 4, where the stability, robustness analysis and capabilities of the developed AFTCS method with respect to measurement and modelling errors are also investigated in simulation. Comparisons with a different FTC strategy relying on the SMC are also reported. Finally, Section 5 summarises contributions and achievements of the paper, providing some suggestions for possible further research topics.

## 2. Cart-pole nonlinear model

The dynamic model of a pendulum (or pole) on a cart shown in Fig. 2 is a classical benchmark in systems and control theory.

The interest in this mechanical system is motivated by the similarity between its dynamic properties and those of several real-world engineering applications like, for example, aerospace vehicles during vertical take-off, cranes, and many others.

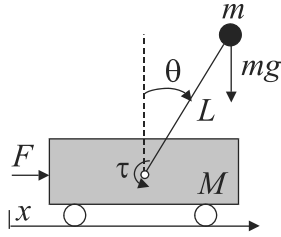


Fig. 2. Scheme of the inverted pendulum on a cart.

Assuming that the cart has mass  $M$ , the pendulum mass  $m$  is concentrated at the tip of a pole of length  $L$ , and that there are no friction effects, the dynamic model obtained using Hamilton's principle is the following:

$$\begin{cases} (M + m)\ddot{x} + mL\ddot{\theta} \cos \theta - mL\dot{\theta}^2 \sin \theta = F, \\ m\ddot{x} \cos \theta + mL\ddot{\theta} - mg \sin \theta = \tau, \end{cases} \quad (1)$$

in which  $g$  is the gravity constant, whilst  $F$  and  $\tau$  are the linear force acting on the cart, and the torque acting directly at the base of the pole, respectively.

If the state variables are

$$X = [x_1 \ x_2 \ x_3 \ x_4]^T = [x \ \dot{x} \ \theta \ \dot{\theta}]^T, \quad (2)$$

and considering  $u = F$  as the control input and  $d = \tau$  as a disturbance, the model can be rewritten in its state-space input affine form as follows:

$$\begin{cases} \dot{x}_1 = x_2, \\ \dot{x}_2 = \frac{mLx_4^2 \sin x_3 - mg \sin x_3 \cos x_3 + u - \frac{d \cos x_3}{L}}{M + m \sin^2 x_3}, \\ \dot{x}_3 = x_4, \\ \dot{x}_4 = \frac{(M + m)g \sin x_3 - mLx_4^2 \sin x_3 \cos x_3}{(M + m \sin^2 x_3)L} - \frac{u \cos x_3 - d/L}{(M + m \sin^2 x_3)L}, \end{cases} \quad (3)$$

As can be seen, the dynamic model of the cart-pole system fulfils the structural requirements described by De Persis and Isidori (2001), concerning the following class of nonlinear systems:

$$\dot{X} = N(X) + G(X)u + P(X)d, \quad (4)$$

where  $N(X)$ ,  $G(X)$  and  $P(X)$  are smooth vector fields. In the following section, the proposed solutions to FDD and AFTC problems, based on the nonlinear geometric approach introduced by De Persis and Isidori (2001), will be developed.

It is worth noting that other types of disturbance terms, different from the torque  $\tau$  signal, can also be considered in (3). As an example, the case of longitudinal  $d_v$

and angular  $d_a$  velocity disturbances can be modelled as

$$\begin{cases} \dot{x}_1 = x_2 + d_v, \\ \dot{x}_2 = \frac{mLx_4^2 \sin x_3 - mg \sin x_3 \cos x_3}{M + m \sin^2 x_3} + \frac{u}{M + m \sin^2 x_3}, \\ \dot{x}_3 = x_4 + d_a, \\ \dot{x}_4 = \frac{(M + m)g \sin x_3 \cos x_3 - mLx_4^2 \sin x_3 \cos x_3}{(M + m \sin^2 x_3)L} - \frac{u \cos x_3}{(M + m \sin^2 x_3)L}. \end{cases} \quad (5)$$

The term  $d_v$  affects only the longitudinal velocity (with the linear position  $x_1$ ), and the longitudinal acceleration does not suffer from this signal. On the other hand, the angular velocity  $x_3$  affects the angular acceleration, which depends on  $d_a$ . However, as these disturbance signals can be easily de-coupled for FDD purposes, as shown in Section 3, only the model (3) with  $d = \tau$  will be taken into account. Moreover, a disturbance described in terms of a torque acting at the base on the pole represents a more realistic situation, since it may be related to the effect of an impact between the pole and some kind of obstacle.

### 3. FDD design and the AFTCS scheme

This section describes the implementation of the FDD scheme and the structure of the AFTCS strategy. Regarding the presented FDD scheme, it belongs to the NLGA framework, where a coordinate transformation, highlighting a sub-system affected by the fault and de-coupled by the disturbances, is the starting point to design a set of adaptive filters. They are able both to detect an additive fault acting on a single actuator and to estimate the magnitude of the fault. It is worth observing that, by means of this NLGA, the fault estimate is de-coupled from disturbance  $d$ .

The proposed approach has been properly applied to the nonlinear model of the system considered in the form

$$\begin{cases} \dot{x} = n(x) + g(x)c + \ell(x)f + p_d(x)d, \\ y = h(x), \end{cases} \quad (6)$$

where the state vector  $x \in \mathcal{X}$  (an open subset of  $\mathbb{R}^{\ell_n}$ ),  $c(t) \in \mathbb{R}^{\ell_c}$  is the control input vector,  $f(t) \in \mathbb{R}$  is the fault,  $d(t) \in \mathbb{R}^{\ell_d}$  the disturbance vector (embedding also the faults which have to be de-coupled, in order to perform the fault isolation) and  $y \in \mathbb{R}^{\ell_m}$  the output vector, whilst  $n(x)$ ,  $\ell(x)$ , the columns of  $g(x)$ , and  $p_d(x)$  are smooth vector fields, with  $h(x)$  being a smooth map.

The model (3) including an additive fault  $f$  can be rewritten in the form

$$\begin{cases} \dot{x}_1 = x_2, \\ \dot{x}_2 = \frac{mLx_4^2 \sin x_3 - mg \sin x_3 \cos x_3 + (u + f)}{M + m \sin^2 x_3} \\ \dot{x}_3 = x_4, \\ \dot{x}_4 = \frac{(M + m)g \sin x_3 - mLx_4^2 \sin x_3 \cos x_3}{(M + m \sin^2 x_3)L} \\ \quad - \frac{d \cos x_3 / L}{(M + m \sin^2 x_3)L}, \end{cases} \quad (7)$$

where, with reference to the input-affine model (6),  $x = [x_1 \ x_2 \ x_3 \ x_4]^T$ ,  $c = u$ , and with

$$n(x) = \begin{bmatrix} x_2 \\ \frac{mLx_4^2 \sin x_3 - mg \sin x_3 \cos x_3}{M + m \sin^2 x_3} \\ x_4 \\ \frac{(M + m)g \sin x_3 - mLx_4^2 \sin x_3 \cos x_3}{L(M + m \sin^2 x_3)} \end{bmatrix} \quad (8)$$

and

$$g(x) \equiv \ell(x) = \begin{bmatrix} 0 \\ 1 \\ \frac{\cos x_3}{L(M + \sin^2 x_3)} \end{bmatrix}. \quad (9)$$

Moreover,  $p_d(x)$  is defined as

$$p_d(x) = \begin{bmatrix} 0 \\ \frac{\cos x_3}{L(M + m \sin^2 x_3)} \\ 0 \\ \frac{1}{L^2(M + \sin^2 x_3)} \end{bmatrix}. \quad (10)$$

The design of the strategy for the diagnosis of the fault  $f$  with disturbance de-coupling, by means of the NLGA considered, is organised as follows:

- computation of  $\Sigma_*^P$ , i.e., the minimal conditioned invariant distribution containing  $P$  (where  $P$  is the distribution spanned by the columns of  $p_d(x)$ );

- computation of  $\Omega^*$ , i.e., the maximal observability codistribution contained in  $(\Sigma_*^P)^\perp$ ;
- if  $\ell(x) \notin (\Omega^*)^\perp$ , the fault detectability condition, the fault is detectable and a suitable change of coordinates can be determined.

$\Sigma_*^P$  can be computed by means of the following recursive algorithm:

$$\begin{cases} S_0 = \bar{P}, \\ S_{k+1} = \bar{S} + \sum_{i=0}^m [g_i, \bar{S}_k \cap \ker \{dh\}], \end{cases} \quad (11)$$

where  $m$  is the number of inputs,  $\bar{S}$  represents the involutive closure of  $S$ ,  $[g, \Delta]$  is the distribution spanned by all vector fields  $[g, \tau]$ , with  $\tau \in \Delta$ , and  $[g, \tau]$  is the Lie bracket of  $g$  and  $\tau$ .

It can be shown that, if there exists a  $k \geq 0$  such that  $S_{k+1} = S_k$ , the algorithm (11) stops and  $\Sigma_*^P = S_k$  (De Persis and Isidori, 2001).

Once  $\Sigma_*^P$  has been determined,  $\Omega^*$  can be obtained by exploiting the following algorithm:

$$\begin{cases} Q_0 = (\Sigma_*^P)^\perp \cap \text{span} \{dh\}, \\ Q_{k+1} = (\Sigma_*^P)^\perp \cap \sum_{i=0}^m [L_{g_i} Q_k + \text{span} \{dh\}], \end{cases} \quad (12)$$

where  $L_g \Gamma$  denotes the codistribution spanned by all co-vector fields  $L_g \omega$ , with  $\omega \in \Gamma$ , and  $L_g \omega$  is the derivative of  $\omega$  along  $g$ .

If there exists an integer  $k^*$  such that  $Q_{k^*} = Q_{k^*+1}$ ,  $Q_{k^*}$  is indicated as o.c.a.  $((\Sigma_*^P)^\perp)$ , where the acronym o.c.a. stands for the *observability codistribution algorithm*.

It can be shown that  $Q_{k^*} = \text{o.c.a.}((\Sigma_*^P)^\perp)$  represents the maximal observability codistribution contained in  $P^\perp$ , i.e.,  $\Omega^*$  (De Persis and Isidori, 2001). Therefore, with reference to the model (6), when  $\ell(x) \notin (\Omega^*)^\perp$ , the disturbance  $d$  can be de-coupled and the fault  $f$  is detectable.

As mentioned above, the examined NLGA to the fault diagnosis problem, described by De Persis and Isidori (2001), is based on a coordinate change in the state space and in the output space,  $\Phi(x)$  and  $\Psi(y)$ , respectively. They consist of a surjection  $\Psi_1$  and a function  $\Phi_1$  such that  $\Omega^* \cap \text{span} \{dh\} = \text{span} \{d(\Psi_1 \circ h)\}$  and  $\Omega^* = \text{span} \{d\Phi_1\}$ , where

$$\begin{cases} \Phi(x) = \begin{pmatrix} \bar{x}_1 \\ \bar{x}_2 \\ \bar{x}_3 \end{pmatrix} = \begin{pmatrix} \Phi_1(x) \\ H_2 h(x) \\ \Phi_3(x) \end{pmatrix}, \\ \Psi(y) = \begin{pmatrix} \bar{y}_1 \\ \bar{y}_2 \end{pmatrix} = \begin{pmatrix} \Psi_1(y) \\ H_2 y \end{pmatrix} \end{cases} \quad (13)$$

are (local) diffeomorphisms, whilst  $H_2$  is a selection matrix, i.e., its rows are a subset of the rows of the identity



matrix. By using the new (local) state and output coordinates  $(\bar{x}, \bar{y})$ , the system (6) is transformed as follows:

$$\begin{cases} \dot{\bar{x}}_1 = n_1(\bar{x}_1, \bar{x}_2) + g_1(\bar{x}_1, \bar{x}_2) c + \ell_1(\bar{x}_1, \bar{x}_2, \bar{x}_3) f, \\ \dot{\bar{x}}_2 = n_2(\bar{x}_1, \bar{x}_2, \bar{x}_3) + g_2(\bar{x}_1, \bar{x}_2, \bar{x}_3) c \\ \quad + \ell_2(\bar{x}_1, \bar{x}_2, \bar{x}_3) f + p_2(\bar{x}_1, \bar{x}_2, \bar{x}_3) d, \\ \dot{\bar{x}}_3 = n_3(\bar{x}_1, \bar{x}_2, \bar{x}_3) + g_3(\bar{x}_1, \bar{x}_2, \bar{x}_3) c \\ \quad + \ell_3(\bar{x}_1, \bar{x}_2, \bar{x}_3) f + p_3(\bar{x}_1, \bar{x}_2, \bar{x}_3) d, \\ \bar{y}_1 = h(\bar{x}_1), \\ \bar{y}_2 = \bar{x}_2, \end{cases} \quad (14)$$

with  $\ell_1(\bar{x}_1, \bar{x}_2, \bar{x}_3)$  not being identically zero. As described by De Persis and Isidori (2001), in this way the observable subsystem (14), which, if it exists, is affected by the fault and not affected by disturbances and the other faults to be de-coupled, is obtained.

This transformation can be applied to the system (6) if and only if the fault detectability condition is satisfied. The system (6) in the new reference frame can be decomposed into three subsystems (14), where the first one (the so-called  $\bar{x}_1$ -subsystem) is always de-coupled from the disturbance vector and affected by the fault as follows:

$$\begin{cases} \dot{\bar{x}}_1 = n_1(\bar{x}_1, \bar{y}_2) + g_1(\bar{x}_1, \bar{y}_2) c + \ell_1(\bar{x}_1, \bar{y}_2, \bar{x}_3) f, \\ \bar{y}_1 = h(\bar{x}_1), \end{cases} \quad (15)$$

where, as the state  $\bar{x}_2$  in (14) is assumed to be measured, the variable  $\bar{x}_2$  in (15) is considered an independent input denoted by  $\bar{y}_2$ .

In the case of (7), with reference to (6), and recalling (10) and (9), the following is obtained:

$$S_0 = \bar{P} = \text{cl}(p_d(x))$$

$$= \text{cl} \left( \begin{bmatrix} 0 \\ -\frac{\cos x_3}{L(M + m \sin^2 x_3)} \\ 0 \\ 1 \\ \frac{1}{L^2(M + \sin^2 x_3)} \end{bmatrix} \right) \equiv p_d(x). \quad (16)$$

By recalling that  $\ker \{dh\} = \emptyset$ , it follows that  $\Sigma_*^P = \bar{P}$  as  $\bar{S}_0 \cap \ker \{dh\} = \emptyset$ . Thus, the algorithm (11) stops with  $S_1 = S_0 = \Sigma_*^P$ .

On the other hand, in order to solve (12), it is necessary to compute the expression  $(\Sigma_*^P)^\perp = (\bar{P})^\perp$ .

However, it is worth noting that, for the case under investigation, the determination of the codistribution  $(\Sigma_*^P)^\perp = (\bar{P})^\perp$  is enhanced due to the sparse structure of (16). Moreover, by means of (12), the computation of  $(\Sigma_*^P)^\perp = (\bar{P})^\perp$  leads to a codistribution  $\Omega^* = \text{o.c.a.}((\Sigma_*^P)^\perp)$  spanned by exact differentials. Finally, any codistribution  $\Omega$  which is a conditioned invariant contained in  $\bar{P}^\perp$  spanned by exact differentials, with  $\Omega = \text{o.c.a.}((\Omega))$  and  $\ell(x) \notin (\Omega)^\perp$ , can be used to define the coordinate change (13). Therefore, the computation of the maximal observability codistribution is not required.

By observing that

$$(\bar{P})^\perp = \left( \begin{bmatrix} 0 \\ \frac{\cos x_3}{L(M + m \sin^2 x_3)} \\ 0 \\ 1 \\ \frac{1}{L^2(M + m \sin^2 x_3)} \end{bmatrix} \right)^\perp \quad (17)$$

$$= \begin{bmatrix} 1 & 0 & 0 & 0 \\ 0 & 0 & 1 & 0 \\ 0 & 1 & -Lx_4 \sin x_3 & L \cos x_3 \end{bmatrix}$$

and noting that  $\text{span}\{dh\} = I_4$ , from (12) it follows that  $\Omega^* = (\Sigma_*^P)^\perp = (\bar{P})^\perp$  and  $(\Omega^*)^\perp = \Sigma_*^P = \bar{P}$ . The fault in (7) is detectable if  $\ell(x) \notin (\Omega^*)^\perp = \Sigma_*^P = \bar{P}$ . This condition is fulfilled due to the expression of  $\ell(x)$  in (9).

As  $\dim\{\Omega^*\} = 3$  and  $\dim\{\Omega^* \cap \text{span}\{dh\}\} = 3$ , it follows that  $\Phi_1(y) : \mathbb{R}^4 \rightarrow \mathbb{R}^3$ . Moreover, as  $\Omega^* \cap \text{span}\{dh\} = \text{span}\{d(\Psi_1 \circ h)\}$ ,  $H_2 y : \mathbb{R}^4 \rightarrow \mathbb{R}^1$ . Thus, as  $h(x) = I_4 x$ , the surjection  $\Psi(y(x))$  is given by

$$\Psi(y(x)) = \begin{pmatrix} \Psi_1(x) \\ H_2 x \end{pmatrix} = \begin{pmatrix} \begin{bmatrix} x_2 + Lx_4 \cos x_3 \\ x_1 \\ x_3 \\ x_4 \end{bmatrix} \end{pmatrix}, \quad (18)$$

where  $H_2 = [0 \ 0 \ 0 \ 1]$ .

Note that, since  $dh = I_4$ , the diffeomorphism  $\Phi_1(x)$  such that  $\Omega^* = \text{span}\{d(\Phi_1)\}$  is given by

$$\Phi_1(x) = \Psi_1(y(x)) = \Psi_1(x). \quad (19)$$

Hence, the  $\bar{x}_1$ -subsystem state variable is

$$\bar{x}_1 = \begin{bmatrix} \bar{x}_{11} \\ \bar{x}_{12} \\ \bar{x}_{13} \end{bmatrix} = \begin{bmatrix} x_2 + Lx_4 \cos x_3 \\ x_1 \\ x_3 \end{bmatrix}. \quad (20)$$

It is worth observing that only  $\bar{x}_{11}$  is affected by the faults, and that the differentials of  $x_2 + Lx_4 \cos x_3$  span an observability codistribution  $\Omega$  contained in  $P^\perp$  with  $\Omega = \text{o.c.a.}(\Omega)$ . Hence, as previously remarked, in order to estimate the fault, it is possible to use the scalar subsystem defined by the coordinate  $\bar{x}_{11} = x_2 + Lx_4 \cos x_3$ , whose dynamics are defined by

$$\dot{\bar{x}}_{11} = \frac{d(x_2 + Lx_4 \cos x_3)}{dt}, \quad (21)$$

from which, by assuming that the whole state is measured, the NLGA-AF can be computed.

With reference to (15), the NLGA-AF can be designed if the condition of De Persis and Isidori (2001) and the following new constraints are satisfied:

- The  $\bar{x}_1$ -subsystem is independent of the  $\bar{x}_3$  state components.
- The fault is a step function of the time, and hence the parameter  $f$  is a constant to be estimated.
- There exists a proper scalar component  $\bar{x}_{1s}$  of the state vector  $\bar{x}_1$  such that the corresponding scalar component of the output vector is  $\bar{y}_{1s} = \bar{x}_{1s}$  and the following relation holds (Bonfè *et al.*, 2007):

$$\dot{\bar{y}}_{1s}(t) = M_1(t) \cdot f + M_2(t), \quad (22)$$

where  $M_1(t) \neq 0, \forall t \geq 0$ . Moreover,  $M_1(t)$  and  $M_2(t)$  can be computed for each time instant, since they are functions just of input and output measurements. The relation (22) describes the general form of the system under diagnosis.

Under these conditions, the design of the adaptive filter is achieved, with reference to the system model (22), in order to provide a fault estimation  $\hat{f}(t)$ , which asymptotically converges to the magnitude of the fault  $f$ .

The proposed adaptive filter is based on the least-squares algorithm with a forgetting factor (Ioannou and Sun, 1996), and it is described by the following adaptation law:

$$\begin{cases} \dot{P} = \beta P - \frac{1}{N^2} P^2 \check{M}_1^2, & P(0) = P_0 > 0, \\ \dot{\hat{f}} = P \epsilon \check{M}_1, & \hat{f}(0) = 0, \end{cases} \quad (23)$$

with the following equations representing the output estimation and the corresponding normalised estimation error:

$$\begin{cases} \hat{y}_{1s} = \check{M}_1 \hat{f} + \check{M}_2 + \lambda \check{y}_{1s}, \\ \epsilon = \frac{1}{N^2} (\bar{y}_{1s} - \hat{y}_{1s}), \end{cases} \quad (24)$$

where all the involved variables of the adaptive filter are scalar. In particular,  $\lambda > 0$  is a parameter related to the

bandwidth of the filter,  $\beta \geq 0$  is the forgetting factor and  $N^2 = 1 + \check{M}_1^2$  is the normalisation factor of the least-squares algorithm. Moreover, the proposed adaptive filter adopts the signals  $\check{M}_1, \check{M}_2, \check{y}_{1s}$ , which are obtained by means of a low-pass filtering of the signals  $M_1, M_2, \bar{y}_{1s}$  as follows:

$$\begin{cases} \dot{\check{M}}_1 = -\lambda \check{M}_1 + M_1, & \check{M}_1(0) = 0, \\ \dot{\check{M}}_2 = -\lambda \check{M}_2 + M_2, & \check{M}_2(0) = 0, \\ \dot{\check{y}}_{1s} = -\lambda \check{y}_{1s} + \bar{y}_{1s}, & \check{y}_{1s}(0) = 0. \end{cases} \quad (25)$$

Thus, the adaptive filter considered is described by the systems (23)–(25).

It can be proved that the asymptotic relation between the normalised output estimation error  $\epsilon(t)$  and the fault estimation error  $f - \hat{f}(t)$  is the following:

$$\lim_{t \rightarrow \infty} \epsilon(t) = \lim_{t \rightarrow \infty} \frac{\check{M}_1(t)}{N^2(t)} (f - \hat{f}(t)). \quad (26)$$

Moreover, it can be proved that the adaptive filter described by the relations (23)–(25) provides an estimate  $\hat{f}(t)$  that asymptotically converges to the magnitude of the step fault  $f$ . The proofs are similar to those by Castaldi *et al.* (2010) and have been omitted here.

In order to design the NLGA-AF scheme, it is possible to design a 4 NLGA adaptive filter in the form of (23)–(25), allowing estimating the magnitude of a step fault acting on the linear force actuator of the inverted pendulum, as shown in (7).

In order to de-couple the effect of the disturbance  $d$  from the fault estimator, it is necessary to select from the  $\bar{x}_1$ -subsystem the following state component:

$$\bar{x}_{1s} = \bar{x}_{11} = x_2 + Lx_4 \cos x_3. \quad (27)$$

Hence, it is possible to describe the specific expression of the fault dynamics (22). The design of the NLGA-AF for  $f$  is based on

$$\begin{cases} \dot{\bar{y}}_{1s} = M_1 \cdot f + M_2, \\ M_1 = \frac{1 - \cos^2 x_3}{M + m \sin^2 x_3}, \\ M_2 = \frac{mLx_4^2 \sin x_3 - mg \sin x_3 \cos x_3}{M + m \sin^2 x_3} \\ \quad + \frac{(M + m)g \sin x_3 \cos^2 x_3}{M + m \sin^2 x_3} \\ \quad - \frac{mLx_4^2 \sin x_3 \cos^2 x_3}{M + m \sin^2 x_3} \\ -x_4^2 \sin x_3 + \frac{1 - \cos^2 x_3}{M + m \sin^2 x_3} u. \end{cases} \quad (28)$$

It is worth noting that, if the disturbance model (5) had been considered, the matrix  $p_d$  and  $(\bar{P})^\perp$  would have been computed as follows:

$$p(x) = p_d(x) = \begin{bmatrix} 1 & 0 \\ 0 & 0 \\ 0 & 1 \\ 0 & 0 \end{bmatrix} \quad (29)$$

and

$$(\bar{P})^\perp = \begin{bmatrix} 1 & 0 \\ 0 & 0 \\ 0 & 1 \\ 0 & 0 \end{bmatrix}^\perp = \begin{bmatrix} 0 & 1 & 0 & 0 \\ 0 & 0 & 0 & 1 \end{bmatrix}. \quad (30)$$

It is easy to verify that, also in this situation, the condition  $\ell(x) \notin (\Omega^*)^\perp = (\bar{P}) = (\Sigma_*^P)$  still holds. Thus, when both longitudinal and angular velocity disturbance are present, the design of the NLGA-AF is based on the following terms:

$$\begin{cases} M_1 = \frac{1}{M + m \sin^2 x_3}, \\ M_2 = \frac{m L x_4^2 \sin x_3 - m g \sin x_3 \cos x_3}{M + m \sin^2 x_3} \\ \quad + \frac{u}{M + m \sin^2 x_3}. \end{cases} \quad (31)$$

However, only the NLGA-AF described by the system (28) will be considered in the following.

In order to compute the simulation results described in next section, the AFTCS scheme has been completed by means of an optimal state feedback control law, designed on the basis of the linear approximation of the model (3) in a neighbourhood of  $X_o = [x_{1d} \ 0 \ 0 \ 0]^T$ , in which  $x_{1d}$  can be any value. In fact, the linear approximation is independent of  $x_1$ , so that the input vector of the optimal controller can be calculated as  $\tilde{X} = [(x_1 - x_{1d}) \ x_2 \ x_3 \ x_4]$ , and the cart-pole system will be stabilised in the upright position at any linear position reference.

The logic scheme of the integrated adaptive fault tolerant approach is shown in Fig. 3.

With reference to Fig. 3, the following nomenclature and symbols have been used:

- $x_{1d}$ : desired value of the linear position,
- $u$ : actuated input,
- $u_c$ : controlled input,
- $u_l$ : output signal from the optimal controller,
- $y$ : measured outputs,
- $f$ : actuator fault,
- $\hat{f}$ : estimated actuator fault.

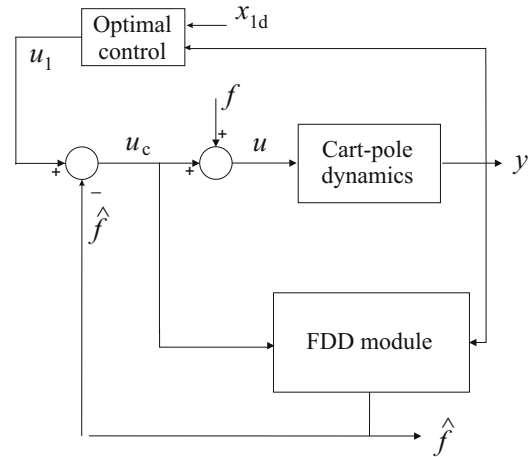


Fig. 3. Logic diagram of the integrated AFTCS strategy.

Therefore, the logic scheme depicted in Fig. 3 shows that the AFTCS strategy is implemented by integrating the FDD module with the existing control system. From the controlled input and output signals, the FDD module provides the correct estimation  $\hat{f}$  of the  $f$  actuator fault, which is injected to the control loop, in order to compensate the effect of the actuator fault. After this correction, the optimal controller provides the exact tracking of the reference signal  $x_{1d}$ .

Regarding the analysis of the stability of the overall AFTCS, the simulation results shown in the following highlight that the model state variables remain bounded in a set, which assures control performance, even in the presence of large fault sizes. Moreover, the assumed fault conditions do not modify the system structure, thus guaranteeing the global stability.

Finally, Section 4 will show the simulation results that have been achieved by implementing the presented integrated FDD and AFTCS strategy.

#### 4. Simulation results

To show the diagnostic characteristics brought by the application of the proposed AFTCS and FDD schemes to the inverted pendulum on a cart, the nonlinear dynamic model of the mechanical system was implemented in Matlab/Simulink®.

The following values of the system parameters were assumed:  $M = 1$  kg,  $m = 0.1$  kg,  $L = 0.3$  m,  $g = 9.81$  m/s<sup>2</sup>.

The optimal controller was designed using the LQR approach in order to minimize the cost function:

$$J = \int_0^{+\infty} (\tilde{X}^T Q \tilde{X} + u R u) dt \quad (32)$$

with  $Q = 10 I_4$  and  $R = 1$ .



In order to show the capabilities of the proposed AFTCS strategy, the system was tested setting as a reference  $x_{1d}$  a square-wave with a 0.2 m amplitude and a 50 sec period.

A random disturbance  $d$  modelled as a zero-mean band-limited noise was applied. It is worth noting that the filter is structurally de-coupled from this disturbance torque, while the measurement noise and the modelling errors may affect the fault estimation.

The following results refer to the simulation of a fault  $f$  modelled as a step signal with a size of 0.1 N, commencing at  $t = 66$  s. Figure 4 shows the estimate of the actuator fault  $\hat{f}$  (solid line), when compared with the simulated actuator fault (dashed line). The fault estimate was achieved by using the logic scheme represented in Fig. 3, and from the FDD module described in Section 3.

As will be shown also in the performance evaluation described in Section 4.1, after a suitable choice of the parameters of the filter (23)–(25), the FDD module provides a quite accurate estimate of the fault size, with a minimal detection delay. Residual errors are due to both the measurement noise and the mismatch between the parameters in the plant and those in the NLGA adaptive filters.

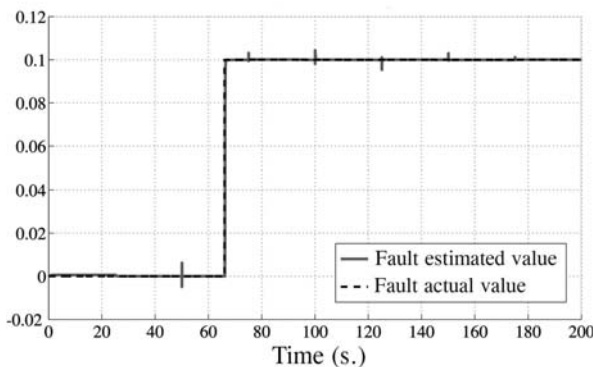


Fig. 4. Real-time estimate  $\hat{f}$  of the actuator fault  $f$ .

Figure 5 shows the cart position  $x_1$  compared with its desired value  $x_{1d}$ . When the fault is not acting on the system, the position error is quite small and is affected mainly by the disturbance torque  $d$ . The fault commences at  $t = 66$  s, but the fault estimate feedback is applied after  $t = 110$  s.

As highlighted in Fig. 5, during the time interval  $66 \text{ s} < t < 110 \text{ s}$ , the steady-state error cannot be eliminated by the optimal controller without the AFTCS. On the other hand, when the proposed AFTCS scheme is switched on, the steady-state error due to the fault is almost zero.

The achieved simulation results summarised in Figs. 4 and 5 show the effectiveness of the presented integrated FDD and AFTCS strategy, which is able to improve the control objective recovery and the reference tracking in the presence of actuator fault. However, the asymptotic

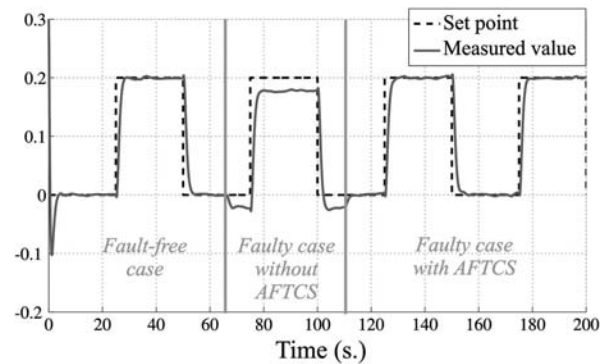


Fig. 5. Linear position  $x_1$  of the cart in the fault-free and faulty cases, with and without the AFTCS.

fault accommodation, the transient and the asymptotic stability of the controlled system, which in this paper are assessed in simulation, require further theoretical studies and investigations.

It is worth observing that the suggested NLGA-AF provides not only the fault detection and isolation, but also the fault estimate. For this reason, it could also be compared e.g., with the fault identification scheme proposed by Kaboré and Wang (2001) or Kaboré *et al.* (2000). However, the proposed NLGA-AF is less sensitive to measurement noise, which allows obtaining a smaller minimal detectable fault. On the other hand, the fault estimation technique of Kaboré and Wang (2001) can provide a faster response and, therefore, a lower detection time.

Note finally that a fault modelled as an additive step function has been considered, since it represents the most used fault situation in connection with the FDD scheme, as reported, e.g., by Edwards *et al.* (2010). Moreover, the FDD module can be easily generalised to estimate, for example, a polynomial function of time, or a generic fault signal belonging to a given class of faults, if the NLGA-AF contains the internal model of the fault itself. Generalisation to more general fault functions is beyond the scope of this paper, and it will be investigated in further works. However, a more realistic fault scenario for the inverted pendulum has been considered in the following. In particular, taking into account also the capabilities of the FDD module considered, the case of an intermittent fault is presented in the following.

Thus, the results refer to the simulation of a fault  $f$  modelled as a sequence of rectangular pulses with variable sizes, commencing at  $t = 66$  s. Figure 6 shows the estimate of the intermittent actuator fault  $\hat{f}$  (solid line), when compared with the simulated actuator fault (dashed line). Also in this case, after a suitable choice of the parameters of the NLGA-AF, the FDD module provides a quite good estimate of the fault signal.

Under this condition, Fig. 7 shows the cart position

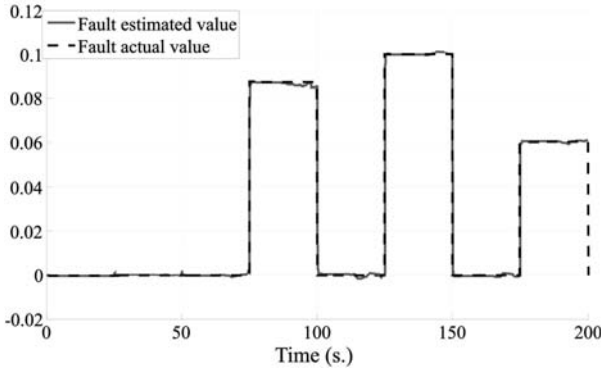


Fig. 6. Real-time estimate  $\hat{f}$  of the intermittent fault  $f$ .

$x_1$  compared with its desired value  $x_{1d}$ . The intermittent fault commences at  $t = 66$  s, but the fault estimate feedback is applied after  $t = 110$  s.

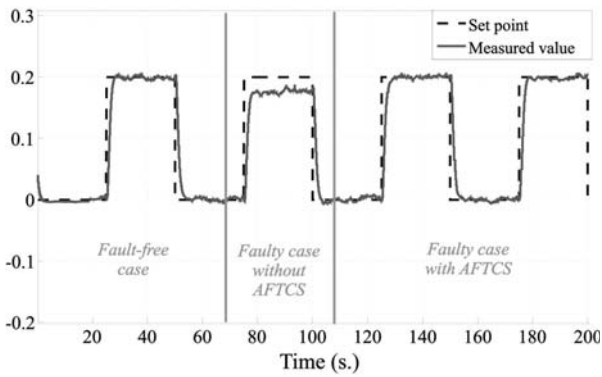


Fig. 7. Linear position  $x_1$  of the cart for the case of an intermittent fault, with and without the AFTCS.

Also for the situation of an intermittent fault, Fig. 7 shows that during the time interval  $66 \text{ s} < t < 110 \text{ s}$  a steady-state error is present, without applying the AFTCS strategy. However, when the AFTCS scheme is working, the steady-state error due to the intermittent fault is almost eliminated.

Therefore, the achieved simulation results highlight that the presented FDD and AFTCS integrated strategy is effective also for the case of intermittent faults with variable amplitudes.

**4.1. Performance evaluation.** In this section, further experimental results are reported. They regard the performance evaluation of the developed AFTCS scheme with respect to modelling errors and measurement uncertainty. In particular, the simulation of different fault-free and faulty data sequences was performed by exploiting the cart-pole benchmark simulator and a MATLAB® Monte Carlo analysis. In fact, the Monte Carlo tool is useful at

this stage as the AFTCS strategy performance depend on the residual error magnitude due to the model approximation as well as on the input-output measurement errors.

In particular, the nonlinear cart-pole simulator developed in SIMULINK® is able to vary the statistical properties of the signals used for modelling both possible process parameter uncertainty and measurement errors. Thus, in this case, Monte Carlo analysis represents a viable method for analysing some properties of the developed AFTCS scheme when applied to the process considered. Under this assumption, Table 1 reports the nominal values of the examined cart-pole model parameters with their uncertainty.

Monte Carlo analysis was performed by describing these variables as Gaussian stochastic processes, with zero-mean and standard deviations corresponding to minimal and maximal error values in Table 1.

Table 1. Simulated cart-pole parameter uncertainties.

Variable	Nominal value	Min. error	Max. error
$M$	1 kg	$\pm 0.1\%$	$\pm 50\%$
$m$	0.1 kg	$\pm 0.1\%$	$\pm 50\%$
$u$	$u_o$	$\pm 0.1\%$	$\pm 25\%$
$y$	$y_o$	$\pm 0.1\%$	$\pm 25\%$
$f$	0	0.1 N	1 N

Moreover, it is assumed that the input and the output signals  $u$  and  $y$  are affected by measurement errors, expressed as percentage standard deviations of the corresponding nominal values  $u_o$  and  $y_o$ , also reported in Table 1.

Thus, for the performance evaluation and robustness analysis of the AFTCS scheme, some indices were used, and thus experimentally evaluated on 500 Monte Carlo runs.

These indices are defined as follows:

**Fault reconstruction relative error,  $\epsilon_{mf}$ :** it represents the mean value of the relative error between the examined fault size  $f$  and the estimated fault size  $\hat{f}$ .

**Reference tracking relative error,  $\epsilon_{mr}$ :** it represents the mean value of the relative error between the reference signal  $x_{1d}$  and the controlled output  $x_1$ .

**Settling time,  $T_{ms}$ :** it represents the mean value of the settling time of the controlled output  $x_1$  with respect to the set-point signal  $x_{1d}$ .

**Fault detection delay,  $\tau_{mf}$ :** it represents the mean value of the time delay required for detecting the considered fault signal.

**Computation time,  $\tau_c$ :** it represents the mean value of the length of the time required to perform the computational process.

**Control signal energy,  $E_{mu}$ :** it represents the mean value of energy of the control input signal  $u$ .

These criteria are computed for several possible combinations of the parameter values reported in Table 1. Table 2 summarises the results obtained by considering the FDD module and the FTC strategy described in Section 3.

Table 2. Monte Carlo analysis for the suggested AFTCS scheme.

Index	Best case	Average case	Worst case
$\epsilon_{mf}$	3%	9%	18%
$\epsilon_{mr}$	13%	14%	15%
$T_{ms}$	18.04 s	18.20 s	18.60 s
$\tau_{mf}$	0.65 s	1.20 s	2.16 s
$E_{mu}$	0.05	0.06	0.07
$\tau_c$	0.015 s	0.017 s	0.019 s

In particular, Table 2 summarises the values of the performance indices considered according to the best, worst and average cases, with reference to the possible combinations of the parameters described in Table 1.

Table 2 shows that, with the proper design of the FDD logic in connection with the FTC scheme, it is possible to achieve reference tracking errors less than 15%, settling times smaller than 19 s, with minimal control input energy, 0.07, low detection delay, and computation time smaller than 0.017 s. The simulations showed that these values are almost independent for the actuator fault size, which varies in the range from 0.1 N. to 1.0 N.

The results demonstrate that Monte Carlo simulation is an effective tool for experimentally testing the design robustness, stability and reliability of the proposed AFTCS method with respect to modelling uncertainty. This last simulation technique example hence facilitates an assessment of the performances of the developed and employed FDD and FTC strategies.

Finally, it is worth noting that, when the case of step fault signals is considered, the perfect knowledge of the system parameters allows settling the optimal threshold logic and therefore providing the analytical estimate of the performance indices (detection time, false alarm rate, etc). On the other hand, when the parameters of the nonlinear model are uncertain, the performance indices are represented by stochastic variables, whose probability distributions can be evaluated only by means of approximations, due to the nonlinearity of the model itself. However, these approximations are not required if the Monte Carlo tool is exploited, since nonlinear maps of stochastic variables do not have to be managed in an analytical way.

**4.2. Comparative studies.** This section provides some comparative results with respect to other FDD and FTC schemes. In particular, advantages and drawbacks of the

AFTCS method suggested in this paper are analysed with respect to the alternative approach, in particular, relying on the SMC.

The SMC can be designed on the basis of a linear or a nonlinear model. In both cases, the design procedure is based on the selection of an appropriate switching manifold, and then on the determination of a control law, including a discontinuous term, which ensures the sliding motion in this manifold. However, SMC design for the nonlinear case is generally applied to systems in the so-called *regular form*, which consists of two blocks: one depending on the control, with the same dimension of the control vector, and the other one independent. Such a regular form may be obtained by means of a nonlinear coordinate transformation. On the other hand, if a linear model is used, the transformation into the regular form and the design of the sliding mode dynamics are simpler, since known results from linear control techniques (i.e., pole placement, eigenstructure assignment, optimal quadratic) are applicable.

Even if the cart-pole benchmark has been studied for SMC design for both its nonlinear model and its linear approximation (Utkin *et al.*, 1999, Par. 4.2 and 5.4), the proposed AFTCS strategy is compared here with SMC design based on Ackermann's formula (Utkin *et al.*, 1999, Par. 5.4). This approach allows determining a state-space discontinuity plane equation in an explicit form, without transforming the original system in a regular form, such that the sliding motions on that plane are governed by linear dynamics with desired eigenvalue placement, independent of disturbances.

This design procedure is therefore inherently fault tolerant, since the disturbance torque and actuator faults are both de-coupled from the sliding motion. The sliding surface based on Ackermann's formula for a linear system  $\dot{x} = Ax + bu$  (with  $A \in \mathbb{R}^{n \times n}$ ) is designed as follows:

$$\begin{aligned} s &= c^T x = 0, \\ c^T &= e^T P(A), \\ e^T &= [0 \dots 0 \quad 1][b \quad Ab \dots A^{n-1}b]^{-1}, \\ P(A) &= (A - \lambda_1 I)(A - \lambda_2 I) \dots (A - \lambda_{n-1} I), \end{aligned} \quad (33)$$

where  $\lambda_1, \lambda_2, \dots, \lambda_{n-1}$  are the desired eigenvalues of the sliding mode. The control law defined as

$$u = -M \text{sign}(s) \quad (34)$$

enforces a sliding motion in the plane  $s = 0$  if

$$M > |c^T Ax| + f_M, \quad (35)$$

where  $f_M$  is an upper bound on an additive disturbance on the control input. In the case of the linearized model of the cart-pole system, such disturbance plays the role of both the disturbance torque and the actuator fault.

In order to provide a brief but clear insight into the above mentioned FDD techniques, the comparison has been performed in the same previous working conditions and based on the indices suggested at the beginning of Section 4.1. It is worth noting that the FTC scheme implemented via the SMC does not exploit the FDD module for fault estimation shown in Fig. 3. In fact, as previously remarked, the SMC strategy is inherently fault-tolerant, as disturbance and fault are de-coupled via the sliding motion. Moreover, the discontinuous control action generated from the SMC, and used by the FDD module, would inevitably worsen the fault reconstruction.

As an example, Fig. 8 shows the linear position  $x_1$  of the cart in the fault-free and faulty cases, when the SMC is used for a step fault situation.

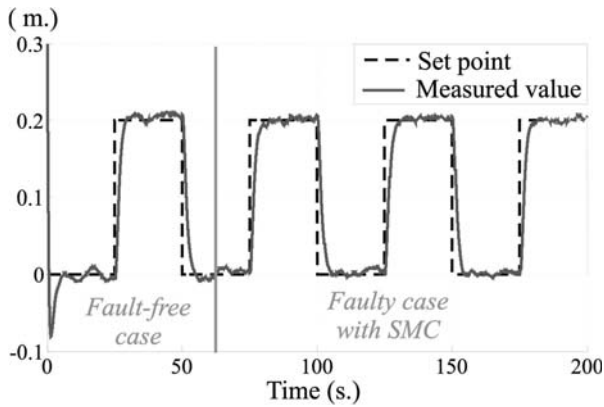


Fig. 8. Linear position  $x_1$  of the cart in the fault-free and faulty cases, with the SMC and for the step fault case.

On the other hand, Fig. 9 depicts  $x_1$  when the SMC is exploited in connection with the intermittent fault case.

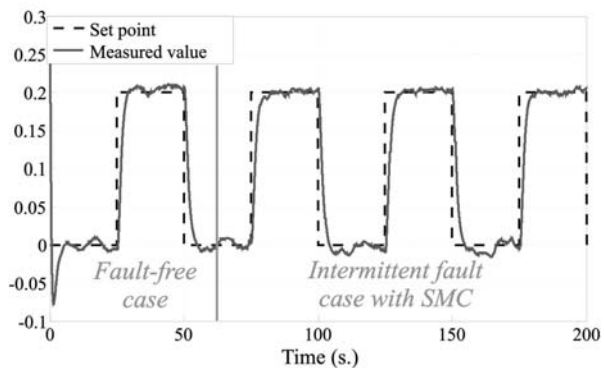


Fig. 9. Linear position  $x_1$  with the SMC and an intermittent fault situation.

Figures 5, 8, and 9 highlight the fact that FTC schemes with different controllers are approximately equally able to accommodate the actuator fault cases considered.

Table 3. Monte Carlo analysis with the sliding mode controller.

Indices	Best case	Average case	Worst case
$\epsilon_{mr}$	9%	10%	11%
$T_{ms}$	20 s	21 s	22 s
$E_{mu}$	20	20.5	20.8
$\tau_c$	0.082 s	0.084 s	0.087 s

However, the comparison between Tables 2 and 3 shows that the FTC scheme using the SMC allows achieving better performances in terms of tracking errors  $\epsilon_{mr}$  and settling times  $T_{ms}$ . However, as reported in Table 3 and depicted in Fig. 10, the control input energy  $E_{mu}$  required by the SMC is much bigger than in the case of the suggested AFTCS, and summarised in Table 2. Moreover, the SMC increases the computational time  $\tau_c$  considerably.

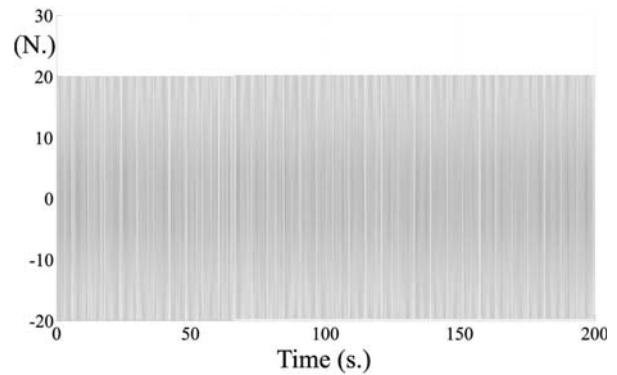


Fig. 10. Control signal activity of the SMC.

As an example, Fig. 10 shows the control signal activity generated by the SMC, which can be compared with the one from the LQR, depicted in Fig. 11.

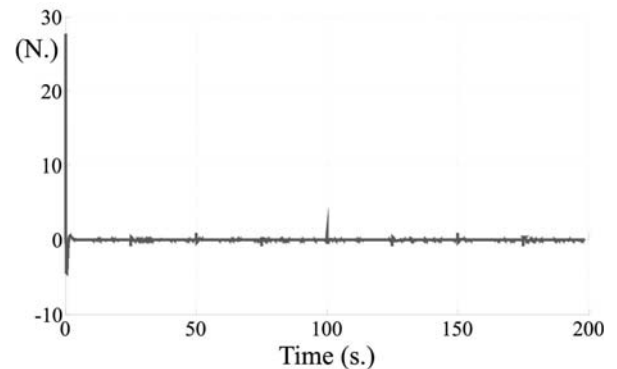


Fig. 11. Control signal from the LQR.

A few comments can be finally drawn here. When the modelling of the dynamic system can be perfectly ob-



tained, the suggested AFTCS allows achieving good performances. This scheme showed also interesting robustness properties in the presence of unmodelled disturbance, modelling mismatch and measurement errors. However, with a scheme relying, e.g., on an SMC, the tracking relative error can fall below the value for the suggested AFTCS scheme. The SMC strategy takes advantage of its intrinsic robustness capabilities, even if with an increased control effort, and an average computation time about 3.59 times bigger than the one required by the suggested AFTCS scheme. However, it represents the time required for computing both the controller and process simulations.

It is worth noting also that the FDD unit was not modified while changing the control strategy. Moreover, one of the advantages of the suggested AFTCS scheme consists in improving the fault tolerance characteristics of those controllers that are not intrinsically fault tolerant. However, for control schemes that are already fault tolerant, the proposed AFTCS method enhances the behaviour of the complete system in transient conditions.

## 5. Conclusion

This paper described the development of an active fault tolerant control scheme which integrates a robust fault diagnosis method with the design of a controller reconfiguration system. The methodology was based on a fault detection and diagnosis procedure relying on disturbance de-coupled adaptive filters designed via the nonlinear geometric approach. The fault tolerant strategy was applied to a classical control design benchmark, namely, the inverted pendulum on a cart, which was simulated in the presence of actuator faults, disturbing forces, measurement noise, and modelling errors.

It is worth observing that the suggested active fault tolerant control was already developed in works by the same authors but applied to aerospace examples. Thus, the contribution of this paper consists in the application of the active fault tolerant control scheme to the well-known benchmark, in order to highlight the computational and mathematical aspects of nonlinear disturbance de-coupling design, which is particularly difficult in the case of the benchmark considered, and hence it can be considered also a tutorial for researchers working in the field of fault detection and isolation as well as fault tolerant control. Note also that, for the first time, the presented disturbance de-coupling problem was solved for the cart-pole system. This represents the first contribution of the paper.

With reference to the achieved performances of the overall fault tolerant control scheme, the advantages and drawbacks of the complete design scheme applied to the nonlinear inverted pendulum example are also discussed and compared with reference to widely used con-

trol strategies. In particular, two schemes were used, namely, linear quadratic and sliding mode controllers. The proposed fault tolerant scheme allows maintaining the existing controller, since a further loop is added to the original scheme, thus ensuring, in the faulty case, the feedback of the fault estimate provided by the nonlinear geometric approach fault diagnosis module. Many applications require not to change or modify the existing controllers.

On the other hand, with reference to the proposed benchmark, the linear quadratic controller is not fault tolerant, while the sliding mode controller presents intrinsic fault tolerant capabilities. Thus, the linear quadratic regulator acquires fault tolerant characteristics when the further loop is implemented. The sliding mode controller, which is already fault tolerant by itself, improves the performance in transient conditions, during the occurrence of faults. This point represents an important feature of the proposed fault tolerant control scheme. The final performances of the developed fault tolerant control strategy are mainly due to the fault estimate that is unbiased thanks to the disturbance de-coupling method.

The stability and robustness of the developed fault tolerant control scheme, together with the evaluation of the achievable performance, are estimated in simulation, by using also the Monte Carlo tool. Results of the numerical simulations show that the proposed active fault tolerant control strategy is robust against disturbances and uncertainties. Comparisons with an alternative fault tolerant control strategy based on a sliding mode controller are also provided. Based on the numerical simulations, the work highlights that the suggested active fault tolerant control strategy exhibits excellent performance in the presence of uncertainties in system parameters. Moreover, the exploited controller shows robust performance in the presence of external disturbances and actuator faults. Thus, the overall design strategy and simulation tool can be regarded as a viable procedure for feasibility analysis of fault tolerant control schemes in achieving prescribed performances, mainly in connection with real applications.

Finally, further investigations will be carried out to evaluate the effectiveness of the suggested approach when applied to real case studies.

## References

- Baldi, P., Castaldi, P. and Simani, S. (2010). Fault diagnosis and control reconfiguration in Earth satellite model engines, *Proceedings of the 9th UKACC International Conference on Control (CONTROL 2010)*, Coventry, UK, pp. 1–6.
- Benini, B., Castaldi, P. and Simani, S. (2009). *Fault Diagnosis for Aircraft System Models: An Introduction from Fault Detection to Fault Tolerance*, 1st Edn., VDM Verlag Dr. Muller, Saarbrücken.
- Bertoni, G., Bertozzi, N., Castaldi, P. and Simani, S. (2010a). A nonlinear guidance and active fault tolerant control system



- for a fixed wing unmanned aerial vehicle, *Proceedings of the 2010 American Control Conference—ACC2010, Baltimore, MD, USA*, pp. 1–6.
- Bertoni, G., Castaldi, P., Mimmo, N. and Simani, S. (2010b). Active fault tolerant control system for a high accuracy planet-image satellite, *Proceedings of the 18th IFAC Symposium on Automatic Control in Aerospace—ACA2010, Nara, Japan*, pp. 1–6.
- Blanke, M., Kinnaert, M., Lunze, J. and Staroswiecki, M. (2006). *Diagnosis and Fault-Tolerant Control*, Springer-Verlag, Berlin.
- Bonfè, M., Castaldi, P., Geri, W. and Simani, S. (2007). Non-linear actuator fault detection and isolation for a general aviation aircraft, *Space Technology—Space Engineering, Telecommunication, Systems Engineering and Control* **27**(2–3): 107–113.
- Castaldi, P., Geri, W., Bonfè, M., Simani, S. and Benini, M. (2010). Design of residual generators and adaptive filters for the FDI of aircraft model sensors, *Control Engineering Practice* **18**(5): 449–495, DOI:10.1016/j.conengprac.2008.11.006.
- Chen, J. and Patton, R.J. (1999). *Robust Model-Based Fault Diagnosis for Dynamic Systems*, Kluwer Academic Publishers, Norwell, MA.
- De Persis, C. and Isidori, A. (2001). A geometric approach to non-linear fault detection and isolation, *IEEE Transactions on Automatic Control* **45**(6): 853–865.
- Ding, S.X. (2008). *Model-based Fault Diagnosis Techniques: Design Schemes, Algorithms, and Tools*, 1st Edn., Springer, Berlin/Heidelberg.
- Edwards, C. (2004). A practical method for the design of sliding mode controllers using linear matrix inequalities, *Automatica* **40**(10): 1761–1769.
- Edwards, C., Lombaerts, T. and Smaili, H. (Eds.) (2010). *Fault Tolerant Flight Control: A Benchmark Challenge*, 1st Edn., Lecture Notes in Control and Information Sciences, Vol. 399, Springer, Heidelberg/Berlin.
- Edwards, C. and Spurgeon, S. (1998). *Sliding Mode Control: Theory and Applications*, 1st Edn., Taylor & Francis, London.
- Ioannou, P. and Sun, J. (1996). *Robust Adaptive Control*, PTR Prentice-Hall, Upper Saddle River, NJ.
- Isermann, R. (2005). *Fault-Diagnosis Systems: An Introduction from Fault Detection to Fault Tolerance*, 1st Edn., Springer-Verlag, Heidelberg/Berlin.
- Kaboré, P., Othman, S., McKenna, T. and Hammouri, H. (2000). An observer-based fault diagnosis for a class of nonlinear systems—Application to a free radical copolymerization reaction, *International Journal of Control* **73**(9): 787–803.
- Kaboré, P. and Wang, H. (2001). Design of fault diagnosis filters and fault tolerant control for a class of nonlinear systems, *IEEE Transactions on Automatic Control* **46**(11): 1805–1810.
- Korbicz, J., Koscielny, J. M., Kowalczyk, Z. and Cholewa, W. (Eds.) (2004). *Fault Diagnosis: Models, Artificial Intelligence, Applications*, 1st Edn., Springer-Verlag, Heidelberg/Berlin.
- Li, H., Zhao, Q. and Yang, Z. (2007). Reliability modeling of fault tolerant control systems, *International Journal of Applied Mathematics and Computer Science* **17**(4): 491–504, DOI: 10.2478/v10006-007-0041-0.
- Mahmoud, M., Jiang, J. and Zhang, Y. (2003). *Active Fault Tolerant Control Systems*, Springer-Verlag, Heidelberg/Berlin.
- Marcos, A., Ganguli, S. and Balas, G.J. (2005). An application of  $H_\infty$  fault detection and isolation to a transport aircraft, *Control Engineering Practice* **13**(1): 105–119.
- Noura, H., Theilliol, D., Ponsart, J.-C. and Chamseddine, A. (2009). *Fault-tolerant Control Systems: Design and Practical Applications*, 1st Edn. Advances in Industrial Control, Vol. 1, Springer, London.
- Rodrigues, M., Theilliol, D., Aberkane, S. and Sauter, D. (2007). Fault tolerant control design for polytopic LPV systems, *International Journal of Applied Mathematics and Computer Science* **17**(1): 27–37, DOI: 10.2478/v10006-007-0004-5.
- Simani, S., Fantuzzi, C. and Patton, R.J. (2003). *Model-Based Fault Diagnosis in Dynamic Systems Using Identification Techniques*, Advances in Industrial Control, Vol. 1, Springer-Verlag, London.
- Slotine, J.-J. and Sastry, S. (1983). Tracking control of non-linear systems using sliding surfaces, with application to robot manipulators, *International Journal of Control* **38**(2): 465–492.
- Su, C.-Y. and Stepanenko, Y. (1994). Adaptive sliding mode control of robot manipulators: General sliding manifold case, *Automatica* **30**(9): 1497–1500.
- Theilliol, D., Join, C. and Zhang, Y. (2008). Actuator fault tolerant control design based on a reconfigurable reference input, *International Journal of Applied Mathematics and Computer Science* **18**(4): 553–560, DOI: 10.2478/v10006-008-0048-1.
- Utkin, V. (1977). Variable structure systems with sliding mode, *IEEE Transactions on Automatic Control* **AC-22**(2): 212–222.
- Utkin, V. (1992). *Sliding Modes in Control Optimization*, Springer-Verlag, Heidelberg/Berlin.
- Utkin, V.I., Guldner, J. and Shi, J. (1999). *Sliding Mode Control in Electromechanical Systems*, 1st Edn., Series in Systems & Control Engineering, Taylor & Francis, London.
- Witczak, M. (2007). *Modelling and Estimation Strategies for Fault Diagnosis of Non-Linear Systems: From Analytical to Soft Computing Approaches*, 1st Edn., Lecture Notes in Control & Information Sciences, Vol. 354, Springer-Verlag, Berlin/Heidelberg.
- Zhang, Y. and Jiang, J. (2008). Bibliographical review on reconfigurable fault-tolerant control systems, *Annual Reviews in Control* **32**(2): 229–252.



**Marcello Bonfè** received his M.Sc. degree in electronic engineering from the University of Ferrara, in 1998, and the Ph.D. degree in information engineering from the University of Modena and Reggio Emilia, Italy, in 2003. Currently, he is an assistant professor of automatic control at the Department of Engineering of the University of Ferrara, Italy. He has published about 50 refereed journal and conference papers. His current research interests include fault detection and isolation, modelling and control of mechatronic systems, and formal verification methods for discrete event systems.



**Paolo Castaldi** was born in Bologna, Italy. He received the *Laurea* degree (*cum laude*) in electronic engineering in 1990 and the Ph.D. degree in system engineering in 1994, both from the University of Bologna, Padova and Firenze. Since 1995 he has been an assistant professor at the Department of Electronics, Computer Science and Systems of the University of Bologna. Since 2009 he has been a member of the IFAC Technical Committee on Aerospace. His research inter-

ests include fault diagnosis and fault tolerant control, adaptive filtering, system identification, and their applications to aerospace and mechanical systems. He is a reviewer of many international journals (awarded as an “outstanding reviewer” of *Automatica* in 2004 and 2005), and an author of about 90 refereed journal and conference papers.



**Nicola Mimmo** was born in San Severo, Italy, in 1983. In 2006 he received his B.Sc. degree in aerospace engineering from the Second University of Naples, Faculty of Engineering, Aversa, Italy, and in 2009 the M.Sc. degree in aerospace and aeronautic engineering from the University of Bologna, Second Faculty of Engineering, Forlì, Italy. He has cooperated with several national and international aircraft and aerospace industries, and is currently a research fellow at the University of Bologna. His research interests include fault diagnosis and fault tolerant control, adaptive filtering, and their applications to aerospace and mechanical systems.



**Silvio Simani** was born in Ferrara, Italy, in 1971. In 1996 he received the *Laurea* degree (*cum laude*) in electrical engineering from the Department of Engineering at the University of Ferrara, and in 2000 the Ph.D. in information science (automatic control) at the University of Ferrara and Modena. Since 2006 he has been an IEEE Senior Member, and from 2000 a member of the SAFEPROCESS Technical Committee. Since 2002 he has been an assistant professor at the Department of Engineering of the University of Ferrara. His research interests include fault diagnosis and fault tolerant control, and system identification. He is the author of about 100 refereed journal and conference papers, as well as two books on the above topics.

Received: 11 March 2010

Revised: 8 January 2011